Preequilibrium proton emission induced by 80 and 120 MeV protons incident on ^{90}Zr

A. A. Cowley, A. van Kent,* J. J. Lawrie, S. V. Förtsch, D. M. Whittal, J. V. Pilcher, and
F. D. Smit
National Accelerator Centre, Faure, 7131, South Africa

W. A. Richter
University of Stellenbosch, Stellenbosch, 7600, South Africa

R. Lindsay and I. J. van Heerden
University of the Western Cape, Bellville, 7530, South Africa

R. Bonetti
Istituto di Fisica Generale Applicata dell'Università di Milano, Italy

P. E. Hodgson
University of Oxford, Oxford OX1 3RH, United Kingdom
(Received 14 August 1990)

Continuum spectra for the inclusive reaction ^{90}Zr(p,p') have been measured for scattering angles between 24° and 145° at incident energies of 80 and 120 MeV. The spectra and angular distributions at various ejectile energies above 20 MeV are compared with published experimental data for ^{90}Zr(p,n) at the same incident energies. Results of statistical multistep direct emission calculations are in excellent agreement with the experimental angular distributions. The extracted strength of the effective nucleon-nucleon interaction is shown to be reasonable with respect to absolute magnitude and energy dependence. A phenomenological parametrization of the angular distributions also describes the experimental quantities well.

I. INTRODUCTION

Recently, the statistical multistep model of Feshbach, Kerman, and Koonin,[1] and Bonetti et al.[2] has been successfully applied to preequilibrium neutrons from (p,n) reactions at incident energies of 80 MeV,[3] and 120 and 160 MeV.[4] These studies indicate a systematic decrease of the effective nucleon-nucleon interaction with increasing incident energy, which is a trend consistent with neutron pickup results[5] and also with theoretical expectation.[6] The work of Scobel et al.[4] is the only investigation above 100 MeV of the reaction mechanism in terms of a statistical multistep direct model, and it is therefore useful to consider also the (p,p') inclusive reaction, which should yield complementary information.

The purpose of the present experiment is to investigate the inclusive reaction ^{90}Zr(p,p') at incident energies of 80 and 120 MeV, and at the same scattering angles as those of Refs. 3 and 4. A theoretical analysis of the (p,p') results in terms of the statistical multistep model in a way designed to be consistent with that applied to the (p,n) reaction, may provide confirmation of existing ideas, and should stimulate further insight. A further justification for exploring the inclusive (p,p') reaction in this incident energy range, where available data are sparse, is that there is an indication[7] that phenomenological parametrizations[8] of continuum angular distributions need to be improved between 100 and 150 MeV. Consequently, there is a need to augment the data which are available to con-

strain the parametrization.

A previous[9] comparison between (p,n) and (p,p') continuum reactions on a variety of target nuclei at an incident energy of 90 MeV indicated that single nucleon-nucleon scattering is an important component of the reaction mechanism. Thus yet another motivation for the present work is to perform a similar comparison for consistency of interpretation at a slightly lower incident energy, as well as at a somewhat higher value.

In Sec. II experimental details are given. In Sec. III a brief summary of the statistical multistep direct emission (SMDE) theory is provided and the calculations are described. The comparison of these experimental data with SMDE theory is discussed and the predictions of a parametrization are given in Sec. IV. Conclusions are presented in Sec. V.

II. EXPERIMENTAL PROCEDURE

The experiment was performed at the cyclotron facility of the National Accelerator Centre, and the equipment, layout, and experimental procedures closely resemble those described in Ref. 10 (and references therein). Continuum energy spectra for the inclusive reaction ^{90}Zr(p,p') were measured at incident laboratory energies of 80 and 120 MeV with an uncertainty of less than 0.5 MeV in absolute beam energy. Energy spectra were recorded for 12 laboratory angles in the range 11°–145°, with angles being chosen to correspond exactly with an-

gles for which (p,n) data[3,4] exist.

The target consisted of a highly uniform ^{90}Zr foil of thickness 10.1 ± 0.2 mg/cm^2, enriched to 97.7% in ^{90}Zr (isotopic impurities include 0.96% ^{91}Zr and 0.71% ^{92}Zr). The detector telescope consisted of two Si (ΔE) detectors of 150 and 1000 μm, respectively, followed by a 75 mm diameter $\times$125 mm thick NaI(Tl) detector. An active collimator (6-mm-thick plastic scintillator) defined a solid angle of 0.578 msr and an angular acceptance of 1.5°. Energy calibration of the Si detectors was based on alpha particles emitted from a ^{228}Th source, while a nonlinear energy calibration for the NaI detector was obtained from the kinematics of elastically scattered protons from hydrogen and carbon (in a thin polythene target). Gain drifts in the photomultiplier tubes of the NaI detectors were monitored by a light-emitting diode pulser system which allowed corrections to be made during analysis. Typical gain drifts of 2 MeV were observed. These pulser peaks could also be used to correct for electronic dead time, which was typically less than 2%.

The beam spot was less than 3 mm in diameter and remained centered on the target to better than 0.5 mm. The angular offset of the beam was measured to an accuracy of 0.2° by comparing elastic-scattering yields on either side of the incident beam.

Halo, which could distort data taken at forward angles, was monitored by frequent comparison of the count rate from an empty frame with that of the rate from the target. Background was less than 1% at 11°, which resulted in no correction being required at larger angles.

Standard electronics and an on-line data-acquisition system were used to record data on tape for subsequent off-line analysis. Corrections[11] for reaction losses in the NaI detector were performed on the ΔE vs E spectra,

with the effect of the particle gate selecting protons being taken into account. At 11° the contribution of the reaction tail of the elastic peak to the continuum was so large that, even with the above corrections, results are considered unreliable and are therefore not presented, while at 24° the correction in the continuum region was of the order of 12% for an incident energy of 120 MeV. Consequently, the correction for reaction losses introduces a relatively small uncertainty in the cross section.

The continuum energy spectra (in the laboratory system) obtained in the present analysis for the ^{90}Zr(p,p') reaction at incident proton energies of 80 and 120 MeV are shown in Fig. 1. The data in Fig. 1 have been compressed to ejectile energy bins of 0.5 MeV, giving a statistical error of less than 2% at half the maximum energy. The overall systematic error is estimated at less than 10%.

III. STATISTICAL MULTISTEP DIRECT THEORY

The multistep direct nuclear reaction code[12] of Bonetti and Chiesa, which is based on the statistical multistep direct emission theory[1,2] (SMDE) of Feshbach, Kerman, and Koonin, was used to calculate double-differential cross sections. The direct emission cross section from a chain of states with at least one particle in the continuum can be expressed as a sum of emission in all the subsequent stages:

$$\frac{d^2\sigma}{dU\,d\Omega} = \frac{d^2\sigma}{dU\,d\Omega}\bigg|_{\text{one step}} + \frac{d^2\sigma}{dU\,d\Omega}\bigg|_{\text{multistep}} . \quad (1)$$

The statistical multistep contribution to the cross section is given by the expression
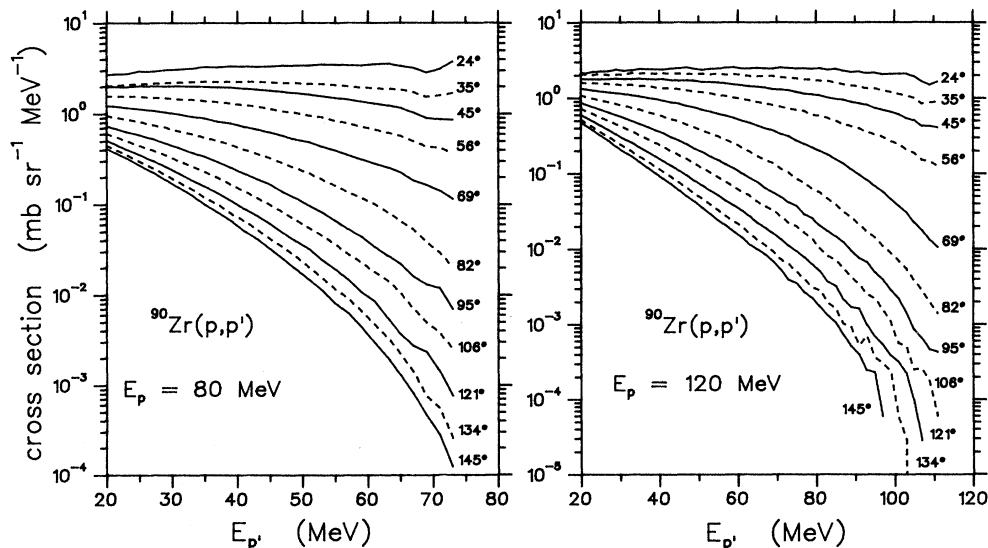

FIG. 1. Experimental energy spectra for the reaction ^{90}Zr(p,p') at incident energies of 80 and 120 MeV for various scattering angles. All quantities are in the laboratory system. Discrete states, which are above the highest displayed ejectile energies, are not included in the plots.

$$\frac{d^2\sigma}{dU\,d\Omega}\bigg|_{\text{multistep}} = \sum_{n=2}^{n_{\max}} \sum_{m=n-1}^{n+1} \int \frac{d\mathbf{k}_1}{(2\pi)^3} \cdots \int \frac{d\mathbf{k}_n}{(2\pi)^3} \left[\frac{d^2W_{m,n}(\mathbf{k}_f,\mathbf{k}_n)}{dU_f\,d\Omega_f}\right] \left[\frac{d^2W_{n,n-1}(\mathbf{k}_n,\mathbf{k}_{n-1})}{dU_n\,d\Omega_n}\right]$$

$$\times \cdots \times \left[\frac{d^2W_{2,1}(\mathbf{k}_2,\mathbf{k}_1)}{dU_2\,d\Omega_2}\right] \frac{d^2\sigma_{1i}(\mathbf{k}_1,\mathbf{k}_i)}{dU_1\,d\Omega_1}, \qquad (2)$$

with $d^2\sigma_{1i}/dU_1\,d\Omega_1$ the cross section for the first collision [see Eq. (5) below].

The $\mathbf{k}_i,\mathbf{k}_n,\mathbf{k}_f$ denote the momenta of the initial, nth intermediate, and final-step nucleon, respectively. The exit mode is labeled by m. The SMDE contribution is calculated to proceed exclusively through stages with one nucleon being unbound. A particular stage n is characterized by the number of particle-hole pairs excited.

The transition probabilities from the $(n-1)$th to the nth stage are given by

$$\frac{d^2W_{n,n-1}}{dU\,d\Omega} = 2\pi^2\rho_c(\mathbf{k}_n)\rho_n(U_n)\langle|v_{n,n-1}(\mathbf{k}_n,\mathbf{k}_{n-1})|^2\rangle, \qquad (3)$$

where

$$v_{a,b}(\mathbf{k}_i,\mathbf{k}_f) = \int \chi_a^{(-)*}(\mathbf{r}_a)\langle\Psi_f|V(\mathbf{r}_a,\mathbf{r}_b)|\Psi_i\rangle\chi_b^{(+)}(\mathbf{r}_b)d\mathbf{r}_a d\mathbf{r}_b. \qquad (4)$$

The density of states of the particle in the continuum is $\rho_c(\mathbf{k}_n)$ for momentum $\mathbf{k}_n$, and $\rho_n(U_n)$ is the level density of the residual nucleus in the nth stage evaluated at the energy U_n. The distorted waves χ are generated from an optical model potential,[13] and the matrix element $v_{n,n-1}$ connects a nuclear state $n-1$ to a state n via an effective N-N interaction $V(r)$. A finite-range Yukawa potential with a range parameter $r_0 = 1$ fm is used for $V(r)$, of which the strength V_0 must be adjusted to reproduce the data. An appropriate energy-averaging procedure[14] brings the matrix element in Eq. (3) to distorted-wave Born approximation (DWBA) form.

Likewise, the first step contribution to the overall double-differential cross section reduces to

$$\frac{d^2\sigma_{1i}}{dU_1\,d\Omega_1} = \sum_L (2L+1)R_2(L)\rho_2(U)\left\langle\frac{d\sigma_L^{(\text{DW})}}{d\Omega}\right\rangle, \qquad (5)$$

where L is the transferred angular momentum and $R_2(L)$ is the spin distribution function, given generally by

$$R_N(L) = \frac{2L+1}{\pi^{1/2}N^{3/2}\sigma^3}\exp\left[\frac{-(L+\frac{1}{2})^2}{N\sigma^2}\right], \qquad (6)$$

and where σ is the spin cutoff parameter, $\rho_2(U)$ the density of 1p-1h states in the nucleus after the first collision of the incident proton, and $N = p + h$ is the number of particles plus holes. The level densities ρ were calculated using the equidistant Fermi-gas model with Pauli corrections and a level-density parameter $a = A/8.5$ MeV^{-1}. In the multistep calculations values must be chosen for the effective interaction strength V_0 and the spin cutoff parameter σ which best reproduce the absolute values as well as the shapes of the experimental angular distributions. The bound single-particle single-hole configurations in the DWBA matrix elements are chosen to be compatible with angular momentum selection rules and energy conservation, and are based on the shell model of the spherical Nilsson potential.

IV. RESULTS

A. Comparison of (p,p') and (p,n) experimental data

Our experiment was designed to produce data which could be directly compared with the ^{90}Zr(p,n) results of Trabandt *et al.*[3] at 80 MeV and Scobel *et al.*[4] at 120 MeV. In general, at both incident energies the (p,n) energy spectra fall off more rapidly with ejectile energy than the (p,p') continuum spectra. At the most forward angle (24°) of our experiment, the shape difference between spectra for the two reactions is very noticeable, as can be seen in the representative examples shown in Fig. 2. Note that in Fig. 2 the results are given in the center-of-
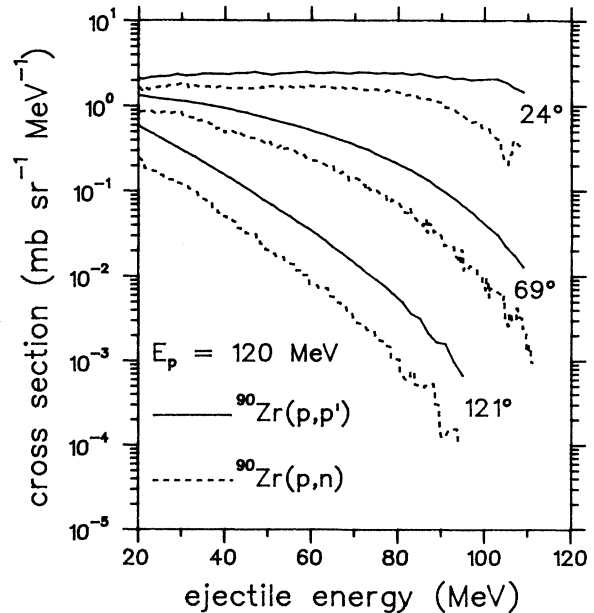

FIG. 2. Comparison between experimental energy spectra for ^{90}Zr(p,p') and ^{90}Zr(p,n) data of Scobel *et al.* (Ref. 4) for selected scattering angles.

mass system as in Refs. 3 and 4.

The angular distributions for the (p,p') reaction are in reasonable shape agreement with those of (p,n), as shown in Fig. 3. The (p,n) angular distributions have been normalized to the (p,p') data at forward angles for display, and these normalization factors vary with ejectile energy, which is just a reflection of the shape differences of the energy spectra as already shown in Fig. 2.

At high emission energies the ratio of (p,n) spectra to the (p,p') data, as indicated in Fig. 3, is in reasonable agreement with the results of Kalend et al.[9] at an incident energy of 90 MeV. However, there appears to be a more rapid falloff in this ratio toward lower ejectile energies.
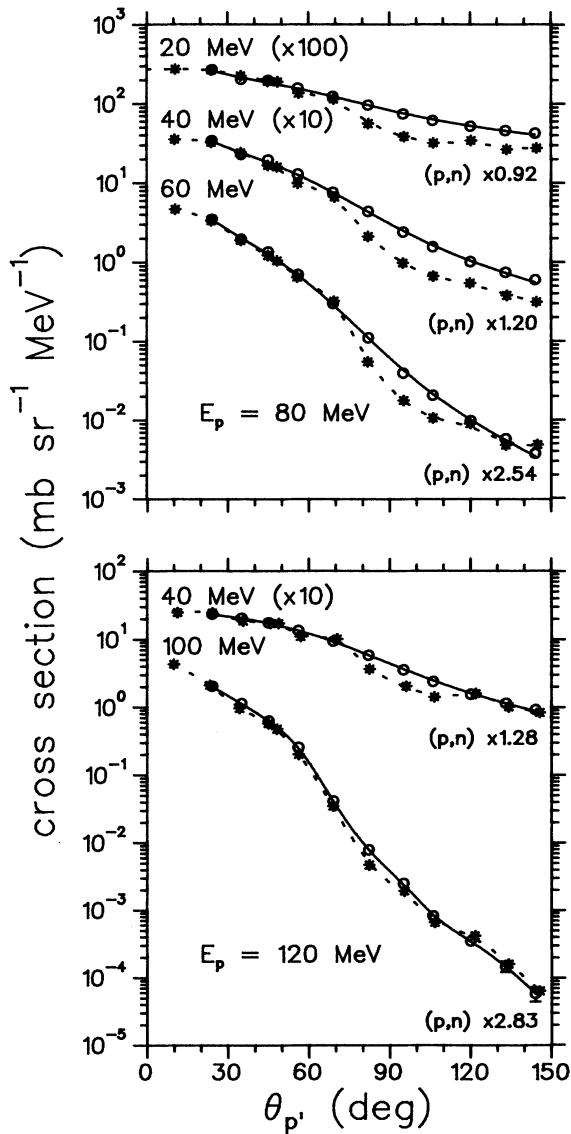
B. Results of statistical multistep direct calculations

Calculated double-differential cross sections as a function of angle for the (p,p') reaction on ^{90}Zr at incident proton energies of 80 and 120 MeV are compared with experimental values in Fig. 4. A remarkable reproduction of the experimental angular distributions has been obtained at both incident energies for all angles and excitation energies, ranging from 20 to 60 MeV at the lower incident energy, and from 20 to 100 MeV at the higher incident energy. For the lowest excitation (highest ejectile) energies, the excellent agreement between theory and experiments extends over more than four orders of mag-
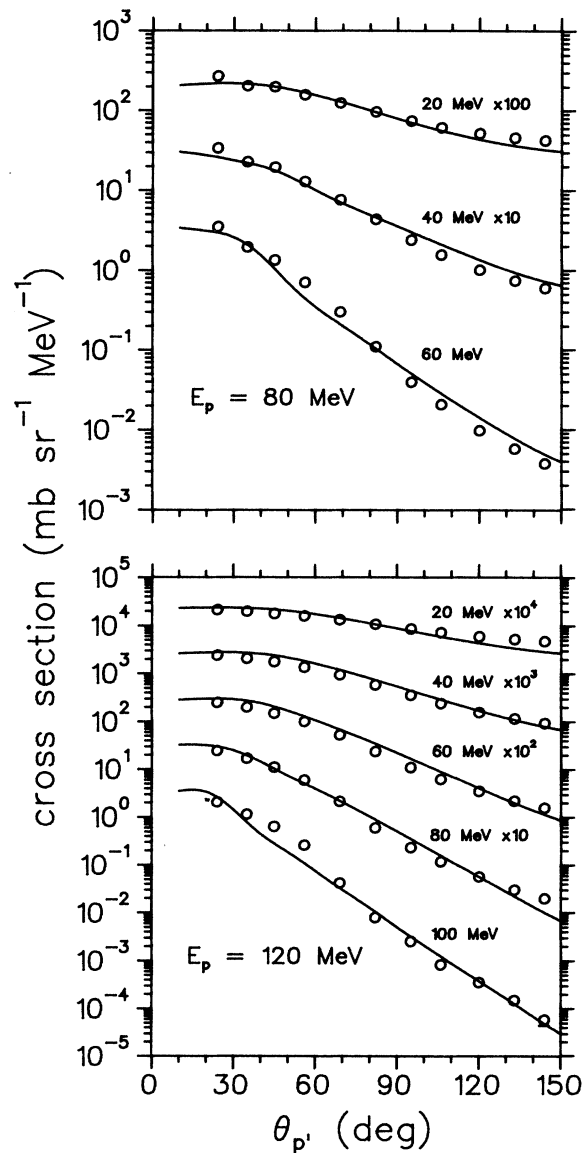

FIG. 3. Comparison between experimental angular distributions at selected ejectile energies for ^{90}Zr(p,p') (circles and solid curves) and ^{90}Zr(p,n) data (asterisks and dashed curves) of Trabandt et al. (Ref. 3) and Scobel et al. (Ref. 4). The (p,n) results have been multiplied by the values as indicated, and curves are drawn to guide the eye.

FIG. 4. Laboratory angular distributions for the reaction ^{90}Zr(p,p') at selected ejectile energies. Statistical error bars are smaller than the symbols of the experimental data. The curves are results of SMDE calculations. Results are multiplied by the factors as indicated for display.

nitude. Similar calculations by Trabandt *et al.*[3] and Scobel *et al.*[4] have been done for (p, n) reactions on the same target and incident energies, and a detailed comparison with these results can be made. Consequently, the results are also of importance in assessing the effects of the ejectile on the multistep processes.

The only parameter varied in our calculations was the two-body effective interaction strength V_0. [The level-density parameter a was taken as 10.5 MeV^{-1}, and the spin cutoff parameter σ was fixed at 2.3. Furthermore, for both incident energies five stages, i.e., $n_{max} = 5$, were used in Eq. (2).] It is of interest to compare our values of V_0 with results of other calculations and to see whether there is a systematic trend as a function of incident energy. The optimal values found for the strength V_0 of the effective interaction were 23 ± 1 MeV for $E_p = 80$ MeV and 17.5 ± 1 MeV for $E_p = 120$ MeV. The corresponding values reported for the (p, n) reaction were 20 ± 1 MeV for $E_p = 80$ MeV (Ref. 3) and 16 ± 1 MeV for $E_p = 120$ MeV,[4] which are reasonably close to the (p, p') values obtained in this work. This comparison between the values of V_0 for (p, p') and (p, n) is meaningful inasmuch as the optical potentials used for protons and neutrons both originate from the same parameter set.[13] More specifically, the proton optical potential is for the best-fit parameter set of Schwandt *et al,*[13] whereas the neutron potential is derived from the same set by changing the sign of the $N - Z$ term. This latter procedure is only correct to a first approximation, and because of the repetitive folding of the (n, n') cross sections in the multistep part of the SMDE calculation, this might reflect itself in the extracted value of V_0.

A monotonic decrease in the residual interaction strength V_0 with projectile energy, as suggested in Ref. 3, is also found in the present calculations (see also Fig. 5). The observed trend in the values of V_0 is consistent with the similar decrease of the real optical potential, which also depends on the strength of the two-body interaction. We can thus estimate the energy variation of V_0 by taking the value $V_0 = 27.9 \pm 3.5$ MeV obtained by Austin[15] from a survey of the analysis of inelastic proton scattering at around 20–50 MeV to discrete final states, and then assume that it has the same energy variation as the real optical potential.

Because the incident particle loses energy as it passes from stage to stage in the multistep process, it would be more precise to allow the effective interaction to increase down the chain. However, it is simpler to use an averaged value, but this effect should be taken into account when comparing the energy dependence of V_0 with that of the optical potential.

An estimate of the magnitude of the effect can be made by assuming that the incident particle loses about half its energy in the first interaction, and that emission from the first and second stages are equally likely.[4] This would reduce the energy-dependent term by about a factor of $\frac{3}{4}$. The real optical potential, normalized to the Austin[15] value of V_0 at 20 MeV, is
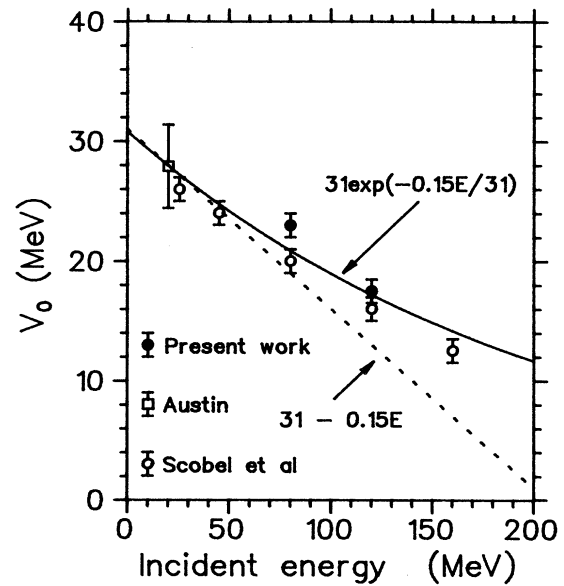
$$V \simeq 34 - 0.2E \ , \tag{7}$$

FIG. 5. Effective interaction strength V_0 as a function of incident energy. Values obtained in this work, together with results of Scobel *et al.* (Ref. 4) and Austin (Ref. 15), are given. Lines indicate expectations obtained from the energy dependence of the optical potential, as discussed in the text.

and allowing for the increase of V_0 down the chain thus gives

$$V \simeq 31 - 0.15E, \tag{8}$$

The empirical values of the effective interaction strength obtained in this work and previously published results[4,15] are plotted in Fig. 5, and these have a similar energy dependence to this function.

More direct evidence of the energy dependence of the effective interaction is provided by the analysis of the $^{90}Zr(p, d)^{89}Zr$ reaction at energies from 20 to 120 MeV by Kosugi and Kosugi.[5] In order to obtain energy-independent spectroscopic factors, they found it necessary to allow the effective interaction to vary with energy. Normalizing their result to that of Austin yields

$$V \simeq 31.5 - 0.12E \ , \tag{9}$$

which is very similar to that given in Eq. (8).

An even better fit to the overall energy dependence can be obtained using the expression found by Johnson, Horen, and Mahaux[16] for neutrons on lead:

$$V = 46.4 \exp[-0.31(E - E_F)/46.4] \ , \tag{10}$$

where E_F is the Fermi energy. Introducing the factor of $\frac{3}{4}$ as before and normalizing gives

$$V \simeq 30.8 \exp(-0.15E/30.8), \tag{11}$$

which is also compared with the empirical values in Fig. 5.

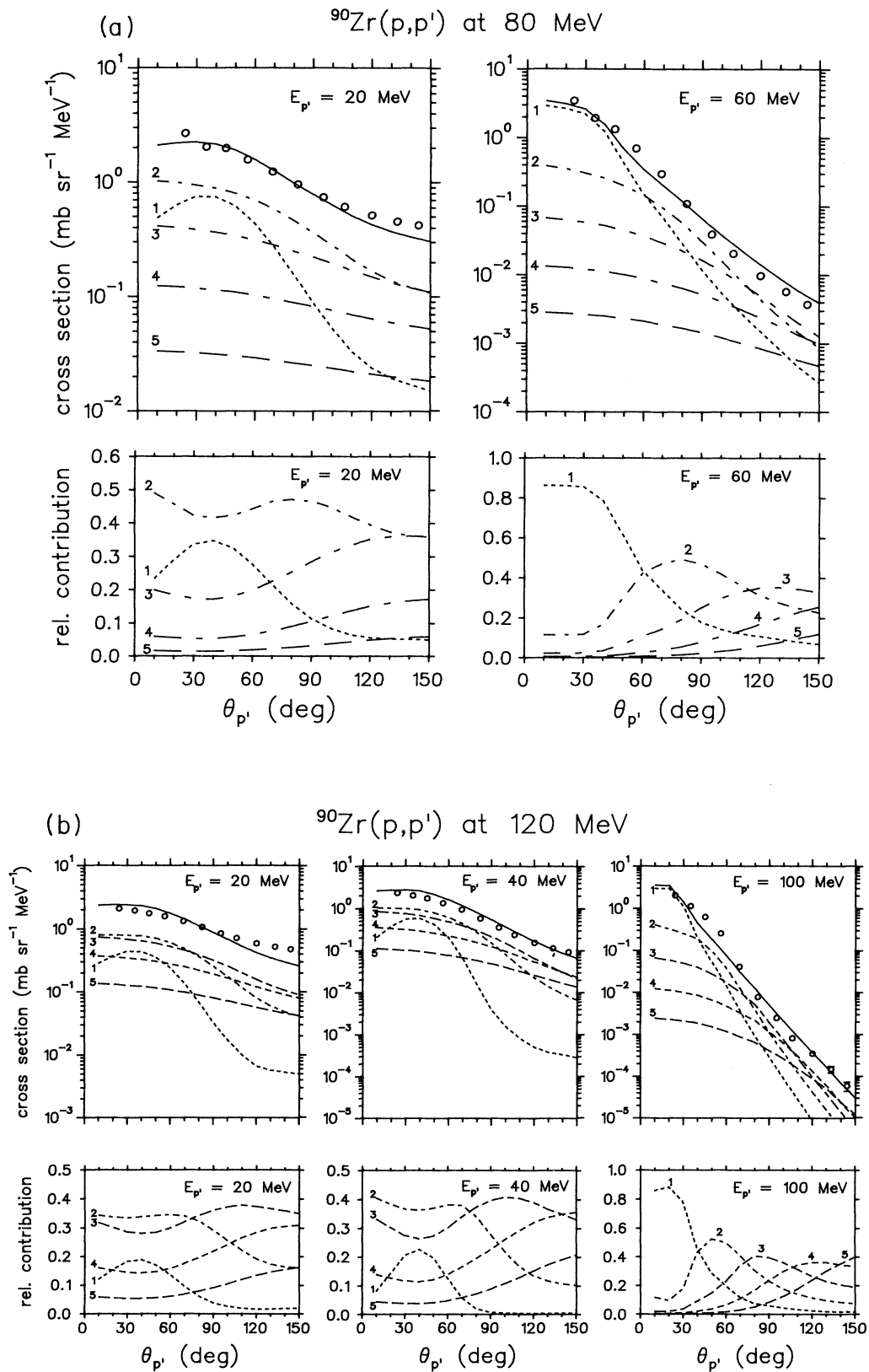In Fig. 5 of Ref. 3 $(E_p = 80.5$ MeV), it is apparent that

FIG. 6. (a) Absolute (upper panels) and relative contributions of the leading five SMDE steps to the angular distribution of 20 and 60 MeV ejectiles from the reaction ^{90}Zr(p,p') at and incident energy of 80 MeV. (b) As in (a) for ejectile energies of 20, 40, and 60 MeV, at an incident proton energy of 120 MeV.

whereas the SMDE calculation gives a very good reproduction of the angular distribution for the lowest neutron energy (22 MeV), the data points for higher ejectile energies are significantly lower in the region of 90°, and this phenomenon is probably related to experimental difficulties[3] only. This systematic deviation is not observed for the (p,p') reaction. In addition, in Fig. 5 of Ref. 4 ($E_p = 120$ MeV), the deviations between experiment and theory appear to be more random, although there still seems to be a region of slightly lower experimental values around 90°. Nothing similar is observed for the (p,p') case, where there is an excellent correspondence between SMDE calculations and experimental cross sections at all proton emission energies.

In Fig. 6 the contributions of the various steps to the double-differential cross section are shown for the two

different incident energies and various exit energies $E_{p'}$. The diagrams for exit energies corresponding to the lowest and highest excitation energies in Fig. 4 of the residual nucleus are included in each case, and also the case with $E_{p'} = 40$ MeV for $E_p = 120$ MeV to facilitate a comparison with the results of Scobel *et al.* (Ref. 4, Fig. 11). The relative contributions of the various steps are also shown in the lower panel of each diagram.

In Fig. 6(a), for $E_p = 80$ MeV, the ejectile energy $E_{p'} = 60$ MeV corresponds to an excitation energy of 20 MeV; the angular distribution for angles up to about 60° can be largely explained in terms of the first step of the SMDE. For larger angles the second step becomes dominant, and subsequent steps become successively more prominent at larger emission angles. At the other extreme of large excitation energy ($E^* = 60$ MeV, with
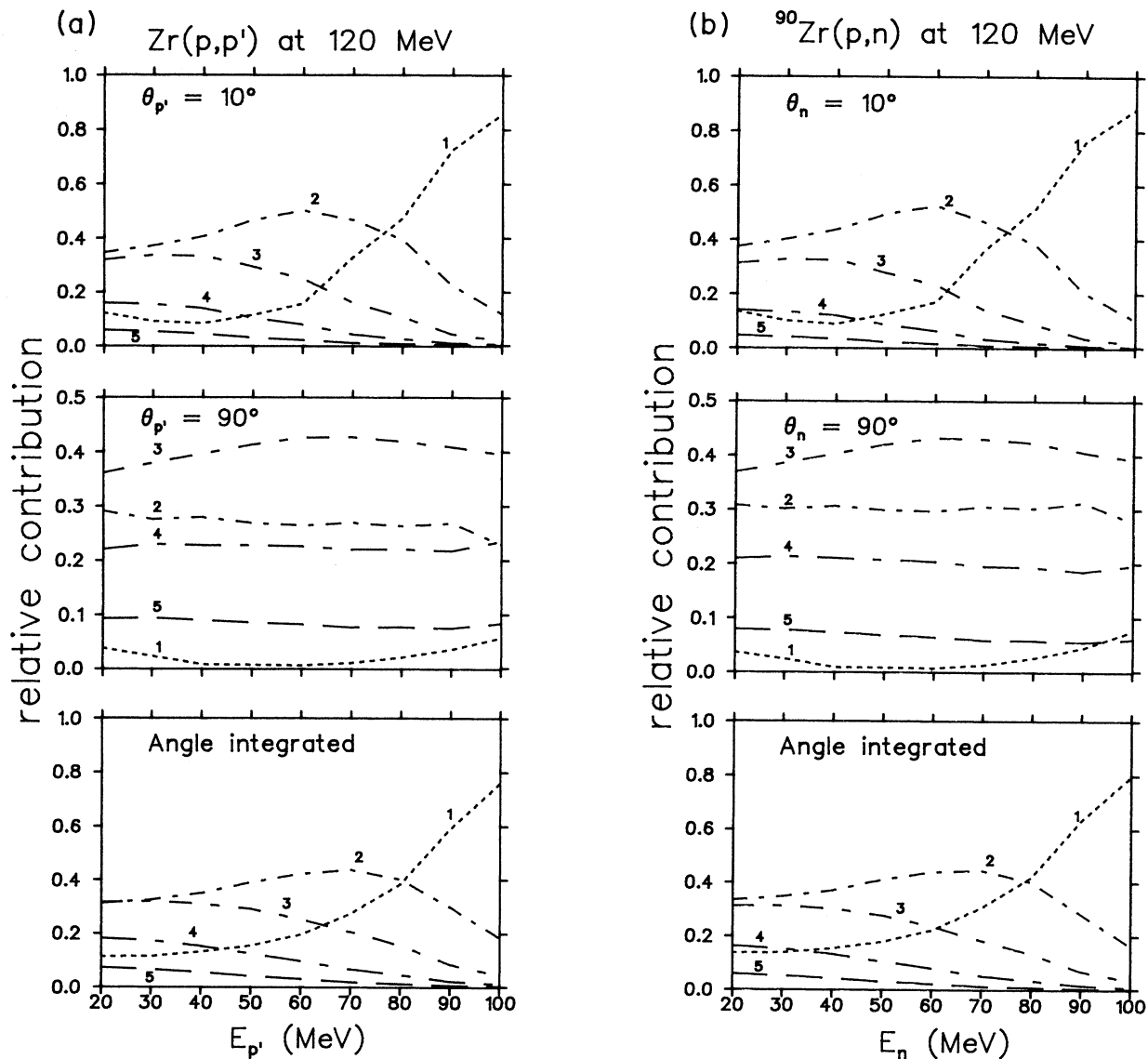

FIG. 7. (a) Relative contributions of the leading five SMDE steps to spectra from ^{90}Zr(p,p') at an incident energy of 120 MeV for scattering angles of 10° and 90°, and the corresponding angle integrated quantities. (b) As in (a) for ^{90}Zr(p,n).

$E_{p'} = 20$ MeV), the first step is never dominant, so that the subsequent more complicated steps play a significant role even at small angles. In Fig. 6(b), for $E_p = 120$ MeV, for the lowest ejectile energy of $E_{p'} = 20$ MeV, a similar trend to that at the lower incident energy is observed, but the first step is comparatively even more suppressed. At an excitation of 20 MeV, we find that at this higher incident energy the first step ceases to be dominant at an even smaller angle (40°). Because the single-scattering angular distribution for a higher-energy ejectile is more forward peaked, scattering at larger angles generally requires the excitation of more complicated configurations

through two or more collisions.

Comparing the (p,p') results in Fig. 6(a) with (p,n) calculations (Ref. 4, Fig. 11) for ejectile energies of 40 and 100 MeV at $E_p = 120$ MeV, we find that the shapes and relative magnitudes of the contributions from the various steps are similar to a very high degree. Although the relative contributions of the successive steps are very similar, the absolute cross sections are higher for (p,p') than for (p,n) at $E_{p'} = 100$ MeV, but not so for $E_{p'} = 40$ MeV. Consequently, we conclude that the difference in the shapes of the energy spectra for (p,p') and (p,n) cannot be ascribed to only a specific step being either more or less prominent.

Figure 7(a) shows examples of theoretical energy spectra for (p,p') at $E_p = 120$ MeV, decomposed in steps as before, for two scattering angles (10° and 90°) as well as angle-integrated spectra. Our calculations for (p,n) with $V_0 = 16$ MeV are shown in Fig. 7(b). Again, the result for (p,p') is qualitatively very similar to the (p,n) result.

The success of the statistical multistep calculations in reproducing angular distributions and angle-integrated spectra depends on the correct proportions of the first- and higher-order step contributions as a function of angle and energy. Our comparison of the (p,p') and (p,n) results has shown that there is a very close correspondence between the two cases as far as the contributions of the various steps to the angular distributions are concerned. The relative contributions to the angle-integrated spectra are also very similar. Furthermore, it should be noted that the present results are in general agreement with the conclusions of Kalend et al.[9] regarding the reaction
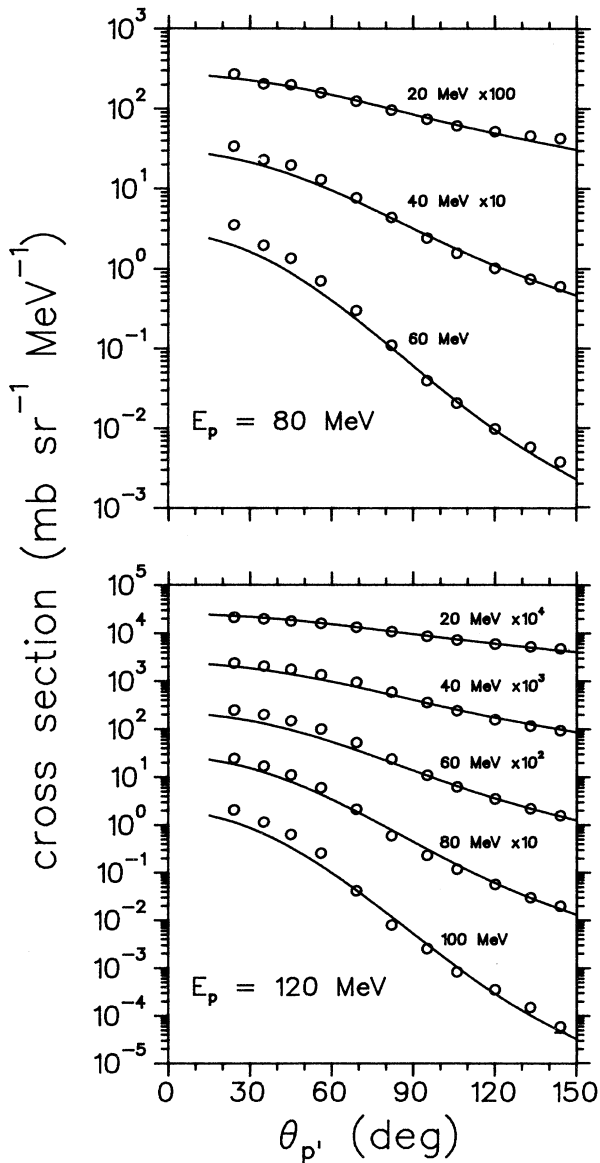

FIG. 8. Laboratory angular distributions for the reaction ^{90}Zr(p,p') at selected ejectile energies. Experimental points are indicated as in Fig. 4. The curves are calculated from the phenomenological parametrization of Eq. (12) as described in the text.
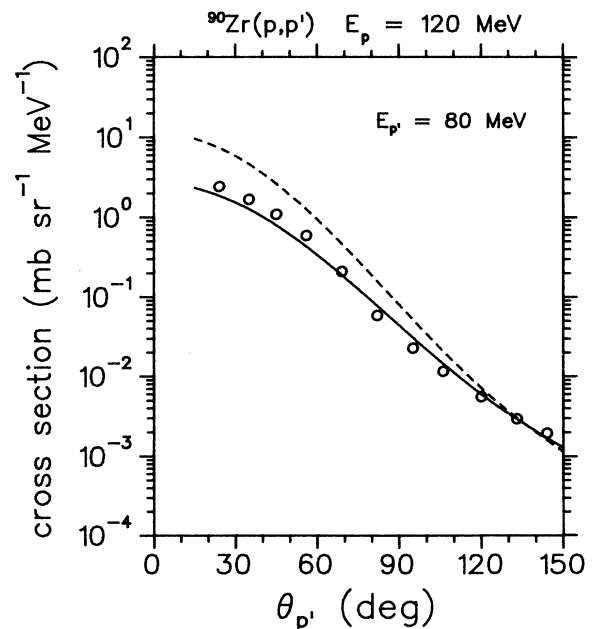

FIG. 9. Laboratory angular distribution for the reaction ^{90}Zr(p,p') at an ejectile energy of 80 MeV. Calculated results are shown for the Kalbach (Ref. 8) parametrization (dashed curve) and the modified formalism of Ref. 7 (solid curve).

mechanism and the relationship between the one-step and multistep components.

C. Phenomenological parametrization
of continuum angular distributions

The parametrization of Kalbach[8] is known to describe continuum angular distributions for various projectiles and ejectiles over a large range of incident energies. The cross section for a purely direct reaction, which should be the dominant component for our data, is given by[8]

$$\frac{d^2\sigma}{d\Omega\,dU}=\sigma_D\frac{\eta}{\sinh\eta}\exp(\eta\cos\theta)\ ,\qquad(12)$$

where θ is the center-of-mass scattering angle, and $4\pi\,\sigma_D$ is the angle-integrated cross section, which is determined in our work by normalizing the calculated values to the experimental data. Below an incident energy of 130 MeV, the slope parameter η is expressed as

$$\eta=\alpha e_b+\beta e_b^3+\gamma e_b^4\ ,\qquad(13)$$

where

$$e_b=E_b+S_b\ .\qquad(14)$$

The emission energy is E_b, and the separation energy S_b is calculated with the liquid-drop model after pairing and shell terms are neglected. The constants α, β, and γ are listed by Kalbach.[8]

In Fig. 8 our experimental data are compared with the prediction of Eq. (12), with η calculated from the Kalbach[8] parametrization for an incident energy of 80 MeV,

and at 120 MeV with the *ad hoc* modification which was found to be required[7] for ^{197}Au(p,p'). This altered formulation of η also gives better agreement with the data than the original value at an incident energy of 120 MeV (Fig. 9).

V. SUMMARY AND CONCLUSIONS

The inclusive (p,p') reaction on ^{90}Zr has been investigated at incident energies of 80 and 120 MeV, and the continuum spectra are found to differ slightly from those of (p,n) at the same incident energies. The features of the experimental angular distributions are in excellent agreement with calculations based on the quantum-mechanical theory of Feshbach, Kerman, and Koonin. The values extracted for the strength of the effective interaction also agree with those found for earlier (p,n) and (p,p') studies. A phenomenological parametrization is also found to have excellent predictive power.

It has been shown that it is possible to reproduce experimental continuum angular distributions accurately with a theory which has a sound foundation. This, in turn, inspires confidence that the theory contains the essential ingredients of the underlying physics. Consequently, this theory may ultimately prove to be a useful tool for obtaining reliable continuum backgrounds in the region of giant resonances, which are conveniently studied in (p,p') and (p,n) reactions at projectile energies above 100 MeV. Extension of these studies to even higher energies and to more complicated reactions is also desirable.

*Permanent address: University of the Western Cape, Bellville, 7530, South Africa

[1]H. Feshbach, A. Kerman, and S. Koonin, Ann. Phys. (N.Y.) **125**, 429 (1980).

[2]R. Bonetti, M. Camnasio, L. Colli Milazzo, and P. E. Hodgson, Phys. Rev. C **24**, 71 (1981).

[3]M. Trabandt, W. Scobel, M. Blann, B. A. Pohl, R. C. Byrd, C. C. Foster, and R. Bonetti, Phys. Rev. C **39**, 452 (1989).

[4]W. Scobel, M. Trabandt, M. Blann, B. A. Pohl, B. R. Remington, R. C. Byrd, C. C. Foster, R. Bonetti, C. Chiesa, and S. M. Grimes, Phys. Rev. C **41**, 2010 (1990).

[5]S. Kosugi and T. Kosugi, Phys. Lett. **127B**, 389 (1983).

[6]M. A. Franey and W. G. Love, Phys. Rev. C **31**, 488 (1985).

[7]A. A. Cowley, S. V. Förtsch, J. J. Lawrie, D. M. Whittal, F. D. Smit, and J. V. Pilcher, Z. Phys. A **336**, 189 (1990).

[8]C. Kalbach, Phys. Rev. C **37**, 2350 (1988).

[9]A. M. Kalend, B. D. Anderson, A. R. Baldwin, R. Madey, J.

W. Watson, C. C. Chang, H. D. Holmgren, R. W. Koontz, J. R. Wu, and H. Machner, Phys. Rev. C **28**, 105 (1983).

[10]J. V. Pilcher, A. A. Cowley, D. M. Whittal, and J. J. Lawrie, Phys. Rev. C **40**, 1937 (1989).

[11]R. E. L. Green, D. H. Boal, R. L. Helmer, K. P. Jackson, and R. G. Korteling, Nucl. Phys. **A405**, 463 (1983).

[12]R. Bonetti and C. Chiesa, code MSD, Milan (unpublished).

[13]P. Schwandt, H. O. Mayer, W. W. Jacobs, A. D. Bacher, S. E. Vigdor, M. D. Kaitchuck, and T. R. Donoghue, Phys. Rev. C **26**, 55 (1982).

[14]Y. Holler, A. Kaminsky, R. Langkau, W. Scobel, M. Trabandt, and R. Bonetti, Nucl. Phys. **A442**, 79 (1985).

[15]S. M. Austin, in *The (p,n) Reaction and the Nucleon-Nucleon Force*, edited by C. D. Goodman *et al.* (Plenum, New York, 1980), p. 203.

[16]C. H. Johnson, D. J. Horen, and C. Mahaux, Phys. Rev. C **36**, 2252 (1987).